

Silicate-break galaxies: an efficient selection method of distant ultraluminous infrared galaxies

T. Takagi¹*, C. P. Pearson²

¹ Centre for Astrophysics and Planetary Science, University of Kent, Canterbury, Kent, CT2 7NR

² Japan Aerospace Exploration Agency, Institute of Space and Astronautical Science, 3-1-1 Yoshinodai, Sagamihara, Kanagawa, Japan

ABSTRACT

We present a photometric selection method for ULIRGs in the redshift range of $z = 1 - 2$. We utilize the most prominent spectral feature of ULIRGs, i.e. the silicate absorption feature at $9.7 \mu\text{m}$ and an optimized filter system at mid-infrared wavelengths. These ‘silicate-break’ galaxies could be selected by using colour anomalies owing to the silicate absorption feature around $9.7(1+z) \mu\text{m}$. Such filter systems are available on the *Spitzer Space Telescope* but we suggest that the most promising selection criteria would be given with mid-infrared bands of *ASTRO-F* satellite due to a more comprehensive set of filter bands than that of *Spitzer*. We study the selection method of silicate-break galaxies with the SED model of both starbursts and quiescent star-forming galaxies, and then verify the method by using the observed spectra of nearby galaxies. We would expect that about 1000 candidates of silicate-break galaxies could be detected per square degree in current and future mid-infrared surveys. The silicate-break selection criteria will break the degeneracy between various galaxy evolution models for extragalactic source counts and place strong limits on the star formation activity at $z = 1 - 2$. Applying our silicate-break technique to initial *Spitzer* results we have tentatively identified the first candidate silicate-break galaxy at $z = 1.6$.

Key words: galaxies: starburst – dust, extinction – infrared: galaxies – submillimetre.

1 INTRODUCTION

Extreme examples of high-redshift counterparts of nearby Ultra-Luminous Infra-Red Galaxies (ULIRGs, (Sanders & Mirabel 1996)) have been found by observations with SCUBA (the Submillimetre Common-User Bolometer Array) at $850\mu\text{m}$ (e.g. Smail et al. (1997), Hughes et al. (1998)). The star formation rates (SFRs) of submillimetre (submm) galaxies are estimated to be more than $10^3 M_{\odot} \text{ yr}^{-1}$ (e.g. Smail et al. (2002), Chapman et al. (2003)), i.e. significantly higher than that of nearby ULIRGs. The observed flux at submm wavelengths is insensitive to the classical flux-redshift relation at $z \gtrsim 1$, owing to the so-called negative K-correction. Nevertheless, the redshift distribution of submm galaxies seems to be rather narrow with a median redshift of ~ 2.4 (Chapman et al. (2003)). A tentative detection of strong clustering within the submm population suggests that submm galaxies may be the progenitors of today’s giant elliptical galaxies (Blain et al. (2004)). A further clue to the evolutionary link between submm galaxies and ellipticals is presented by the Spectral Energy Distribution (SED) fitting analysis by Takagi et al. (2004).

Spheroids contain about 50 – 70 % of the stellar mass in the local universe (e.g Schechter & Dressler (1987), Fukugita, Hogan, & Peebles (1998)). It is not yet clear whether the formation of such a large mass fraction can be explained by submm galaxies alone, including the recently found optically-faint radio galaxies at similar redshifts (Chapman et al. 2004), which could have the similar SFR with that of submm galaxies. The SFR density due to submm galaxies and optically-faint radio galaxies has a strong peak at $z = 2 - 3$ (Chapman et al. 2004), which corresponds to the time-scale of only ~ 1 Gyr.

Recent studies on near-IR selected galaxies in the HDF-N (Dickinson et al. 2003) and the HDF-S (Fontana et al. 2003) show that a significant fraction of stars at the present epoch are formed at $z = 1 - 2$, i.e. at later epochs than when most of submm galaxies are found. Therefore, ULIRGs at $z = 1 - 2$ could be a key galaxy population in understanding the formation process of spheroidal galaxies as well as submm galaxies at $z \gtrsim 2$. Furthermore it is probable that these infrared galaxies are the main contributors to the cosmic infrared background (c.f. Chary & Elbaz (2001)). Such galaxies will be prime targets of new infrared satellites, such as *Spitzer* (Werner et al. 2004) and *ASTRO-F* (Pearson et al. 2004), (Murakami 1998).

* E-mail: t.takagi@kent.ac.uk

interesting high- z objects, such as Lyman-break galaxies (Steidel et al. 2003), massive galaxies at high redshifts (van Dokkum et al. 2004; Cimatti et al. 2004), Lyman- α emitters at $z \gtrsim 4$ (Cowie & Hu 1998; Taniguchi et al. 2003; Shimasaku et al. 2003), have revolutionized the field of the galaxy evolution at high redshift. These techniques are widely used to select objects for spectroscopy, and for statistical studies to derive luminosity functions and spatial correlation functions, which require a large sample at a similar redshift.

Until now, these photometric pre-selection techniques have been developed for galaxy populations observed at optical and near-infrared (NIR) wavelengths. Similar techniques for selecting luminous infrared galaxies at $z = 1 - 2$ are strongly demanded. Recently, the spectroscopic bump at $1.6 \mu\text{m}$ due to the H^- opacity minimum has been applied to galaxies detected at $24 \mu\text{m}$ with *Spitzer* (Le Floc'h et al. 2004; Egami et al. 2004). This technique requires coordinated surveys at NIR wavelengths targeting the rest-frame $1.6 \mu\text{m}$ and MIR wavelengths to detect significant dust emission, and also unambiguous cross-identification between NIR and MIR sources, which is not easy for blended pairs of NIR sources (e.g. Egami et al. 2004). Therefore, any techniques using only the dust emission would be more efficient.

In the spectra of ULIRGs, the most prominent features are found at MIR wavelengths, i.e. silicate absorption at $9.7 \mu\text{m}$ and the PAH features. Here, we investigate the possibility of selecting luminous infrared galaxies at $z \gtrsim 1$ with *Spitzer* and *ASTRO-F* by focusing on the MIR features. We hereafter refer to distant infrared galaxies selected by this method as ‘silicate-break’ galaxies for simplicity. Note that Charmandaris et al. (2004) briefly discuss the possibility of estimating redshifts from the MIR features by using the Infrared Spectrograph (IRS, Houck et al. (2004)) peak-up imagers at 16 and $22 \mu\text{m}$ onboard *Spitzer*, although it is difficult to use these imagers for large area blank field surveys, because of the small field-of-view.

Silicate-break galaxies could be selected by using the colour anomaly owing to the silicate absorption feature around a $9.7(1+z) \mu\text{m}$ band. For example, a galaxy with the SED of Arp 220 at $z = 1.5$ would be too faint to be detected with *Spitzer* in the MIPS $24 \mu\text{m}$ band, while it would be detectable in the other infrared bands, as shown in Figure 1. Thus, sources which are detected in all the *Spitzer* bands but $24 \mu\text{m}$ are candidates for heavily obscured galaxies at $z = 1.5$. With the sensitivity of *Spitzer* and *ASTRO-F*, most of the silicate-break galaxies would be classified as ULIRGs.

The structure of this paper is as follows. In section 2 we describe the SED model used to derive the selection criteria for silicate-break galaxies. In section 3 we discuss the selection criteria for the *Spitzer* and *ASTRO-F* infrared satellite missions and predicted effectiveness of the filter combinations in detecting potential silicate-break candidates. The potential number of silicate-break galaxies at $z = 1 - 2$ are estimated using two infrared evolutionary models in section 4. We give discussion and conclusions in section 5. Throughout this work we assume a flat cosmology of $\Omega_m = 0.3$, $\Omega_\Lambda = 0.7$, and $H_0 = 75 \text{ km sec}^{-1} \text{ Mpc}^{-1}$.

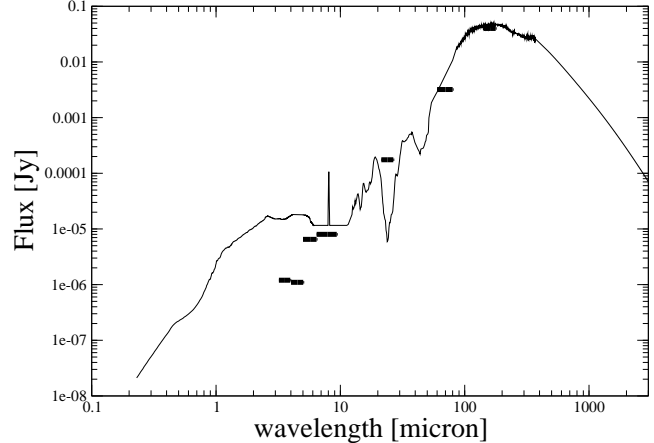


Figure 1. An example of a potential silicate-break galaxy. The SED of Arp220 (Elbaz et al. 2002) at $z = 1.5$ is compared with the 5σ detection limits at *Spitzer*/IRAC bands and MIPS $24 \mu\text{m}$ achieved in the Lockman Hole region (Huang et al. 2004; Floc'h et al. 2004). At 70 and $160 \mu\text{m}$, we adopt the confusion limit based on the MIPS observations (Dole et al. 2004). With these detection limits, galaxies with the SED of Arp220 are detectable at all the *Spitzer* bands, except for $24 \mu\text{m}$. Note that the luminosity is assumed to be twice of Arp220.

2 SED TEMPLATES

In order to derive the colour criteria to select silicate-break galaxies in a desired redshift range only, we need to ensure that there is negligible contamination from the other redshifts by using a wide variety of possible SEDs.

We adopt the evolutionary SED model of starbursts by Takagi et al. (2003a), in which the SED variation is explained by the difference in the starburst age and the compactness of the starburst region Θ . It is found that the SED model reproduces not only the SED of ULIRGs, but also the SED of UV-selected starburst galaxies which are usually less luminous. This means that the SED model is capable of covering the wide variation of observed starburst galaxy SEDs.

In Takagi et al. (2003a), three types of dust model are adopted, i.e. the Milky Way (MW), Large Magellanic Cloud (LMC), and Small Magellanic Cloud (SMC) dust models (see Takagi et al. 2003b for details of the models). The fraction of silicate dust grains is assumed to increase from the MW to SMC model, i.e. as a function of the metallicity. Therefore, the silicate absorption feature is most prominent in the SEDs described by the SMC type dust model. Thus, in this work, we focus on the SMC dust model, which is found to be suitable for most of the nearby ULIRGs modelled by Takagi et al. (2003a). We have confirmed that none of the SED models with the MW and LMC type dust causes any contamination in the selection criteria discussed below.

We constrain the possible parameter space of the SED model, suitable for high- z ULIRGs by using the observed SED variation of submm galaxies. Note that the SED model itself can cover a wide variety of starburst SEDs, including that of UV-selected starburst galaxies, i.e. non-ULIRGs. We first constrain the starburst age at $t/t_0 \geq 1$ where t_0 is the evolutionary time-scale of starbursts, since the probability to select very young galaxies is low. We use the models younger than $t/t_0 = 6$, which are enough to reproduce the majority

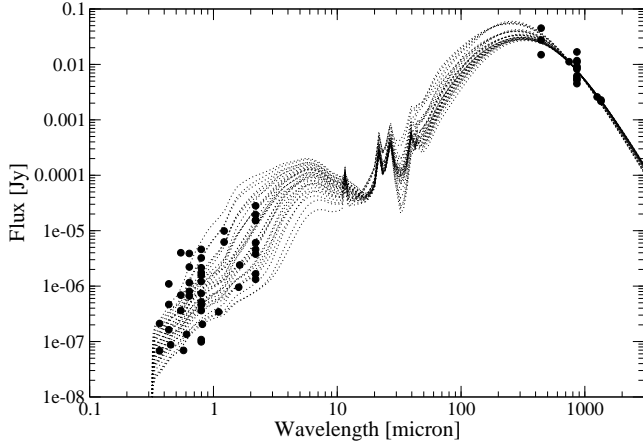


Figure 2. The SED models with $t/t_0 = 1 - 6$ and $\Theta = 0.6 - 1.4$ adopted from Takagi et al. (2004). The SMC dust model is adopted. The SEDs are normalized with $S_{850} = 8$ mJy at $z = 2.5$. The observed fluxes of submm galaxies (solid circles) are summarized in Takagi et al. (2004).

of observed SEDs (Takagi et al. 2003a; Takagi et al. 2004). We then constrain the compactness Θ to $0.6 - 1.4$, which is enough to cover the observed range of SEDs of submm galaxies. In Figure 2, we show the SED models with the starburst age of $t/t_0 = 1 - 6$, and $\Theta = 0.6 - 1.4$, together with the observed fluxes of submm galaxies at $z = 2 - 3$. The SED models are normalized at $S_{850} = 8$ mJy at $z = 2.5$. We adopt an initial mass function (IMF) with a power-law index of $x = 1.10$, which is slightly flatter than the Salpeter IMF ($x = 1.35$), following Takagi et al. (2004). Note that submm galaxies which are very faint at optical – NIR wavelengths, are not included in the sample. Such galaxies could be more heavily obscured than the coverage of the SED model, and would therefore have an even deeper silicate absorption feature.

Using the high- z galaxy sample, rather than well studied nearby galaxies, to constrain the SED parameter space has two distinct advantages; 1) the redshift of the target galaxies themselves is high ($z > 1$), and 2) the effect of any underlying stellar population will be minimal in the optical – NIR in the observed frame. Note that the latter advantage is useful in estimating the variation of the SED parameters from the observed optical – NIR SEDs. SED analysis of individual submm galaxies is given in Takagi et al. (2004).

We also need an SED template for quiescent star-forming galaxies to estimate any possible contamination of the sample of silicate-break galaxies. We adopt the phenomenological SED template of Dale et al. (2001), which reproduces the empirical spectra and infrared colour trends. In this model, SEDs are characterized by a power-law index α of the distribution of dust mass over a wide range of interstellar radiation field strengths. We use the SED models with $\alpha \geq 1.25$ which are suitable for the quiescent population.

Both of SED templates by Takagi et al. (2003a) and Dale et al. (2001) do not include the contribution of AGN. AGN generally produce a featureless continuum which can be approximated by a power-law spectrum without PAH emission (e.g. Laurent et al. 2000). This means that the presence of an AGN will decrease the prominence of the silicate absorption feature. Such AGN-dominated galaxies

would be difficult to be selected as silicate-break galaxies even with high luminosity. Therefore, the *number* of silicate-break galaxies depends on how strong the AGN contribution is in ULIRGs at $z \sim 1.5$. However, the AGN contribution is not very important to derive the *selection criteria* of silicate-break galaxies, since AGN-dominated galaxies have almost constant MIR colours, owing to the power-law like spectrum. This is confirmed below by using observed spectra of AGN in section 3.3.

All fluxes are calculated using the transmission curves at each filter band. The digital form of the transmission curves of *Spitzer* bands and *ASTRO-F* bands are available from the web page of Spitzer Science Center (SSC) and H. Matsuura (2004, private communication), respectively, except for the *Spitzer*/IRS filters at the time of writing. For the IRS filters at 16 and 22 μm , we assume box car profiles for the transmission curve.

3 SELECTION CRITERIA OF SILICATE-BREAK GALAXIES

3.1 Case for *Spitzer*

Spitzer covers the near to far-infrared range in 7 bands at 3.6, 4.5, 5.8, 8.0 μm with the IRAC instrument (Fazio et al. 2004) and 24, 70, 160 μm with the MIPS instrument (Rieke et al. 2004). Also, the IRS has peak-up imagers at 16 and 22 μm , although the field-of-view is small. These imagers would be useful for targeted observations of objects which are too faint to obtain spectroscopic redshifts. In Figure 3, we show the three flux ratios, 8-to-24 μm , 24 to 70 μm and 16 to 22 μm as a function of redshift for the SED templates described above, where fluxes are given per unit frequency (i.e. flux density).

For the 8 to 24 μm flux ratio, the colour bump around $z = 1.5$ due to silicate absorption is not prominent. The flux ratio can vary with a rather large scatter at different redshifts, which makes the silicate-break selection difficult. This is because the stellar light mainly contributes to the 8 μm flux, while dust emission contributes at 24 μm . Also, note that quiescent star-forming galaxies at $z < 0.5$ have a similar flux ratio to that of ULIRGs at $z \sim 1.5$. Obviously, this flux ratio is not useful for the selection of silicate-break galaxies.

We can expect a weaker variation of the flux ratio as a function of redshift, when the dust emission contributes in both the selected bands. This is the case for the flux ratio of 24 to 70 μm for the *Spitzer* band. From the flux variation predicted by the SED model, galaxies with $\log(f_{24}/f_{70}) \lesssim -1.7$ could be silicate-break galaxies at $z \sim 1.5$. This selection is effective for galaxies with relatively deep silicate absorption feature. This means that 24-to-70 μm selection is likely to be biased towards high optical depth. The contamination from quiescent star-forming galaxies is negligible.

With the IRS peak-up imagers at 16 and 22 μm , we could make more complete sample of silicate-break galaxies than that of 24-to-70 μm selection, i.e. free from the bias in optical depth. If we adopt the criterion of $\log(f_{16}/f_{22}) \gtrsim -0.1$, most of the SED templates of ULIRGs satisfy this criterion at $z = 1 - 2$. Although this selection suffers from some contamination from quiescent star-forming galaxies

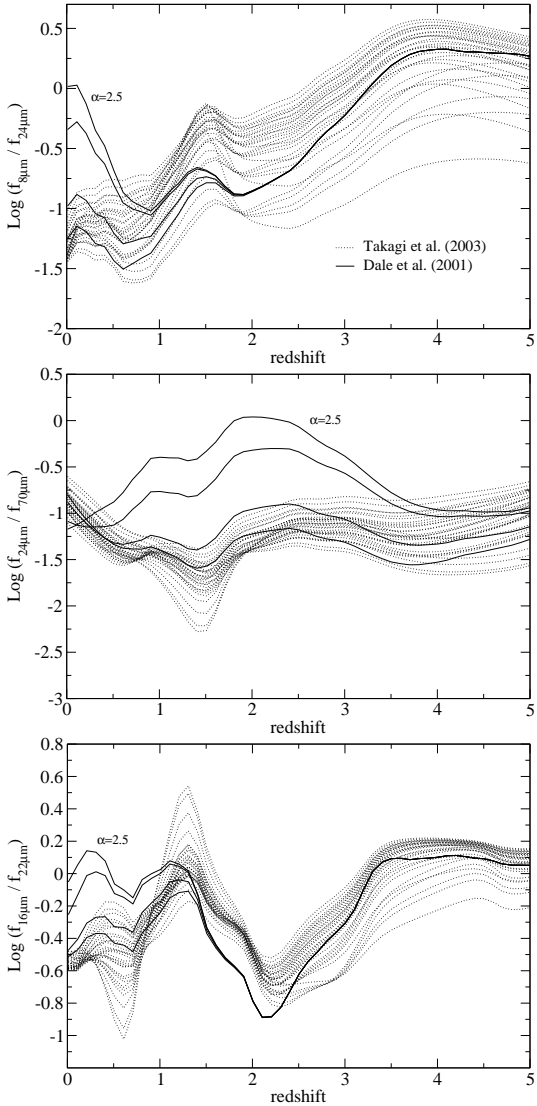


Figure 3. The flux ratios with *Spitzer* bands as a function of redshift. Dotted lines indicate the SED models by Takagi et al. (2003a), shown in Figure 2. Thin solid lines indicate the SED template by Dale et al. with $\alpha = 1.25, 1.5, 2.0$, and 2.5 . The model with $\alpha = 2.5$ (coolest one) is indicated explicitly.

with cold dust temperatures at $z < 1$, it can be removed by using additional photometry at $70\,\mu\text{m}$. In Figure 4, we show the colour-colour diagram with the two IRS imagers and $70\,\mu\text{m}$. The 22 -to- $70\,\mu\text{m}$ ratio is higher for more quiescent galaxies, which is distinguishable from that of ULIRGs at $z = 1 - 2$. The selection with the 16 -to- $22\,\mu\text{m}$ ratio also includes ULIRGs at $z > 3$, which are interesting objects as well. The fraction of such high- z ULIRGs would be small with the current sensitivity limits.

3.2 Case for *ASTRO-F*

ASTRO-F has a more comprehensive set of photometric bands at MIR wavelengths, compared to *Spitzer*. The Infra Red Camera (IRC) instrument on *ASTRO-F* has 3 channels each comprising of 3 photometric bands (Wada et al. (2003)). The IRC-NIR has bands at $2.4, 3.2, 4.3\,\mu\text{m}$. The

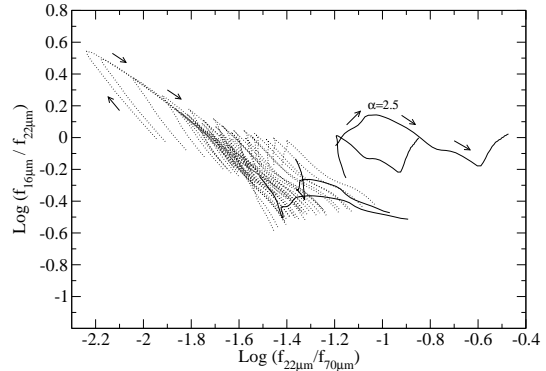


Figure 4. The separation of silicate-break galaxies and low- z quiescent star-forming galaxies. Dotted lines indicate the colours of ULIRGs at $z = 1 - 2$. Solid lines are for quiescent star-forming galaxies at $z < 1$. Arrows indicate the direction of the change in colours with increasing redshift. The model of Dale et al. with $\alpha = 2.5$ (coolest one) is indicated explicitly.

IRC-MIR-S has bands at $7, 9, 11\,\mu\text{m}$. The IRC-MIR-L has bands at $15, 20, 24\,\mu\text{m}$. The bands at 9 and $20\,\mu\text{m}$ are considerably wider than the others. Thus among the three channels of the IRC, the MIR-L channel has the most useful bands to cover the silicate absorption in galaxies at $z > 1$; i.e. $15\,\mu\text{m}$ (L15), wide $20\,\mu\text{m}$ (L20W), and $24\,\mu\text{m}$ (L24).

In Figure 5, we show three flux ratios as a function of redshift. The flux ratio of L24 to L20W has the most prominent colour bump at $z \sim 1.5$ due to the silicate absorption. Galaxies with $\log(f_{\text{L24}}/f_{\text{L20W}}) \lesssim 0$ could be silicate-break galaxies. In this colour cut, most of the galaxies showing the silicate absorption feature could be selected, irrespective of the optical depth. As in the case of the selection with the IRS peak-up imagers, there would be some contamination from quiescent star-forming galaxies with cold dust temperatures at $z < 1$. Again, this contamination can be removed with additional photometry at FIR wavelengths as shown in Figure 6. Also note that this selection will include a small fraction of ULIRGs at $z > 3$.

3.3 Test with observed spectra

Takagi et al. (2003b) perform a detailed comparison of the SED model with the observations of Arp220 and M82. They find that the depth of the silicate absorption features in Arp220 and M82, along with the UV-submm SED, are reproduced by the SMC and LMC dust models, respectively. The detailed observed spectra of silicate absorption features are slightly different from that of the model, which can be attributed to the uncertainty of the optical properties of dust grains. Also note that some ULIRGs show strong absorption features of molecules, such as CO gas and water ice (Spoon et al. 2004), which are not taken into account in the models. Thus, we need a test of derived selection criteria by using observed spectra.

Here we test our selection criteria by using 8 observed spectra obtained with *ISO* and *Spitzer*, i.e. Arp220, M82 (Elbaz et al. 2002), NGC1068 (Sturm et al. 2000), IRAS F00183-7111 (Spoon et al. 2004a), NGC4418 (Spoon et al. 2004b), UGC5101, Mrk1014, and Mrk463 (Armus et al.

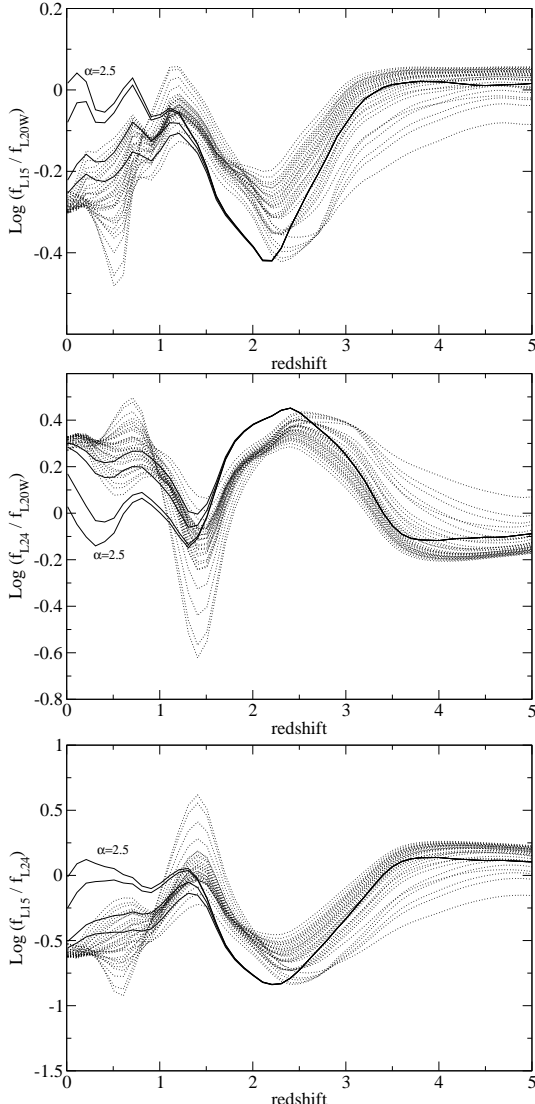


Figure 5. The flux ratios with *ASTRO-F* bands as a function of redshift. The same line style is used as in Figure 3.

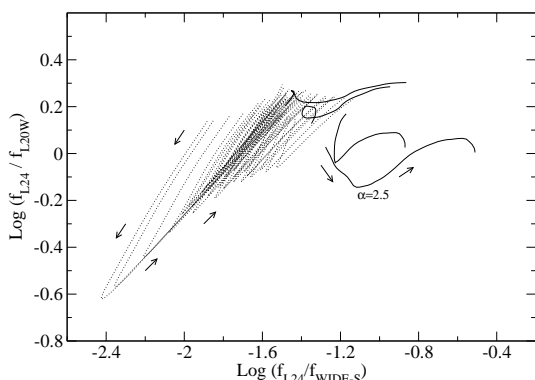


Figure 6. The same as Figure 4, but for *ASTRO-F* bands. The WIDE-S band is the wideband filter at 80 μm .

2004)¹. Among these galaxies, AGN-continuum dominates the MIR emission in NGC1068 (typical Seyfert 2), Mrk1014 (infrared luminous QSO) and Mrk463 (Seyfert 2). Both NGC4418 and IRAS F00813-7111 have strong silicate absorption features, although the strong radio emission indicate the presence of AGN. By nature, this sample is not complete in any statistical sense.

In Figure 7, we show the 16-to-22 μm flux ratio for *Spitzer* and the L24-to-L20W for *ASTRO-F* as a function of redshift based on the observed spectra. The selection criteria based on the model analysis result in the selection of 5 out of 8 galaxies as silicate-break galaxies. As expected, these selections miss the continuum-dominated galaxies, which have almost constant flux ratio and cause no contamination.

Note that the variation of flux ratios are similar to those of the SED models. This suggests that these flux ratios are insensitive to the detailed features in the MIR spectra, such as molecular absorptions. Also, the selection criteria would be less sensitive to any uncertainty in the dust model, such as the detailed shape of silicate feature.

In Charmandaris et al. (2004), there are two galaxies which clearly satisfy the silicate-break selection, i.e. object 9 and 11 in their table. The flux ratio of 16 to 850 μm suggests that the object 11 (CUDSS 14A) is likely to be at $z > 1$. We perform the SED fitting for this galaxy by using the same SED models as those in Takagi et al. (2004). The best-fitting SED model suggests that this galaxy is a silicate-break galaxy at $z = 1.6$ as shown in Figure 8. We suggest that this galaxy is the first promising candidate of a silicate-break galaxy.

4 EXPECTED NUMBER OF SILICATE-BREAK GALAXIES

We use the galaxy evolution models of Pearson (2004) to predict the numbers of silicate-break galaxies expected in the mid-infrared surveys that are or will be conducted by *Spitzer* and *ASTRO-F*. These models use the type dependent luminosity functions derived from the ISO-ELAIS survey (Rowan-Robinson et al. (2004)) of Pozzi et al. (2004) and Matute et al. (2004) to represent the normal and starburst/ULIRG and AGN populations respectively. We investigate two particular models, in order to predict the numbers of silicate-break galaxies. The models are categorized by their dominant populations of starburst (M82 like) and ULIRG (Arp 220 like) sources respectively. The first (starburst dominated) model is referred to as the *Bright End Model*, and broadly follows the evolutionary scenario of Pearson & Rowan-Robinson (1996). This model assumes power law evolution in both luminosity and density of the forms $(1 + z)^k$ for the starburst, AGN and ULIRG populations respectively. The second (ULIRG dominated) model is referred to as the *Burst Model*, and broadly follows the evolutionary scenario of Pearson (2001). This model assumes a similar power law evolution in luminosity, for the starburst and AGN populations and an initial exponential burst +

¹ Since the digital form of the spectra in Armus et al. (2004) is not available to the public, we used the data trace software ‘DataThief II’ for the electric version of the published paper. The error on this process is negligible for our study.

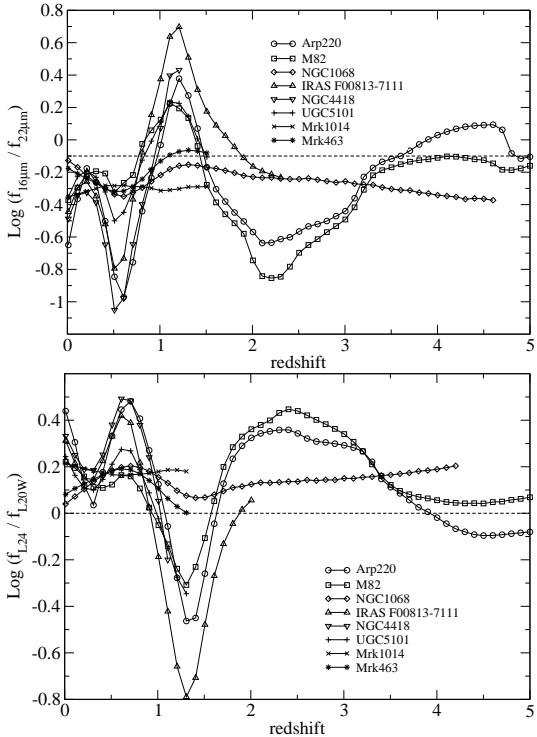


Figure 7. The flux ratios for *Spitzer* band and *ASTRO-F* band expected from the observed spectra of nearby galaxies. Dashed horizontal lines indicate the selection criteria of silicate-break galaxies

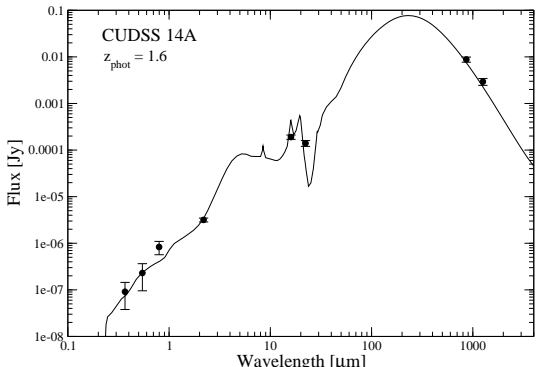


Figure 8. The result of SED fitting for CUDSS 14A. The fluxes at optical-NIR bands, the IRS bands, 850 μm and 1.3 mm are taken from Lilly et al. (1999), Charmandaris et al. (2004), Eales et al. (1999), and Gear et al. (2000), respectively.

power law evolutionary scenario for the ULIRG population. In both models the normal galaxies are assumed to be non-evolving. See Pearson (2004) for details of the models. These models provide good fits to both the 15 μm ISO counts and the *Spitzer* counts at 24 μm (Papovich et al. (2004), Oliver et al. (1997), Aussel et al. (1999), Elbaz et al. (1998), Serjeant et al. (2000)). These model fits are shown in Figure 9.

For the purpose of this study, to model the ULIRG population (i.e. the potential silicate-break galaxies) we have used two SED templates from the library of Takagi (2003a) rather than that of Arp220 which has a rather anomalous

farinfrared-midinfrared ratio. These SEDs are modelled on the local IRAS galaxies, IRAS 15250 and IRAS 12112, for which the model gives an excellent fit to the observed multi-band data, specifically at NIR-submm wavelengths. The SED of IRAS 15250 and IRAS 12112 are assumed to be representative of infrared luminosities of ($L_{IR} \gtrsim 10^{11} L_\odot$) and ($L_{IR} \gtrsim 10^{12} L_\odot$), respectively.

The selection criteria for silicate-break galaxies dictates that the interesting sources will be ULIRGs between $z = 1 - 2$. Hence in Figure 10 we plot the number of sources per square degree as a function of flux at 24 μm in 3 redshift bins of $z = 0 - 1$, $1 - 2$ and $2 - 3$. For the *Spitzer* 24 μm band, the number of potential silicate-break galaxies are predicted to be ~ 900 and ~ 1500 sq.deg for the *Bright End* model and the *Burst* model respectively. All the silicate-break galaxies selected at 24 μm should be detected at the confusion limit of the 70 μm surveys with *Spitzer* (Lonsdale et al. (2003), (2004)).

ASTRO-F will have a more comprehensive set of bands in the mid-infrared, having 3 bands sensitive to the silicate-break galaxies (15, 20, 24 μm) with its' IRC instrument. Present survey strategies for the IRC include both a deep survey and a shallow survey around the north ecliptic pole (NEP) region with the sensitivity of ~ 50 and ~ 170 μJy (5σ) at L20W band, respectively (Pearson et al. (2001), (2004)). The survey area of the deep and the shallow survey would be ~ 0.5 and $\gtrsim 3$ deg 2 , respectively (Pearson et al. (2001), Matsuura & Pearson (2004), Pearson & Matsuura (2004)). For the deep NEP survey similar numbers to the *Spitzer* 24 μm results for the 2 evolutionary models are expected in all 3 bands of the MIR-L since we are effectively detecting all ULIRGs between $z = 1 - 2$ at these depths. For the shallow pointing survey, we predict ~ 400 and ~ 1500 candidates per square degree at 20 μm for the *Bright End* model and the *Burst* model, respectively.

The actual number of silicate-break galaxies would be somewhat smaller than the predicted number of ULIRGs at $z = 1 - 2$, since the possible contribution from the AGN continuum make the silicate absorption less prominent. Note that the fraction of AGN-dominated galaxies, i.e Seyfert 1 and 2, in nearby ULIRGs are $\sim 30\%$ (Sanders & Mirabel 1996). X-ray follow-up observations of deep *ISO* surveys in the HDF-N and the Lockman Hole consistently suggest that $\sim 25\%$ of *ISO*-detected MIR sources are likely to be AGN-dominated (Fadda et al. 2002). X-ray properties of the silicate-break population and other ULIRGs would be very important to study the obscuration of AGNs by dust at high redshifts.

The observed number of silicate-break galaxies will place a strong lower limit on the number of ULIRGs at this redshift range. From the above predictions and our silicate-break selection criteria, it will be possible to discriminate between the models above and more extreme evolutionary models (e.g. Dusty E/S0 models (Xu et al. 2003), cirrus dominated models (Rowan-Robinson 2001)). From Figure 10 it can be seen that even the *Bright End* and *Burst* evolutionary models differ by factors of 2 – 3 in their predictions for ULIRGs between $z \sim 1$ and 2.

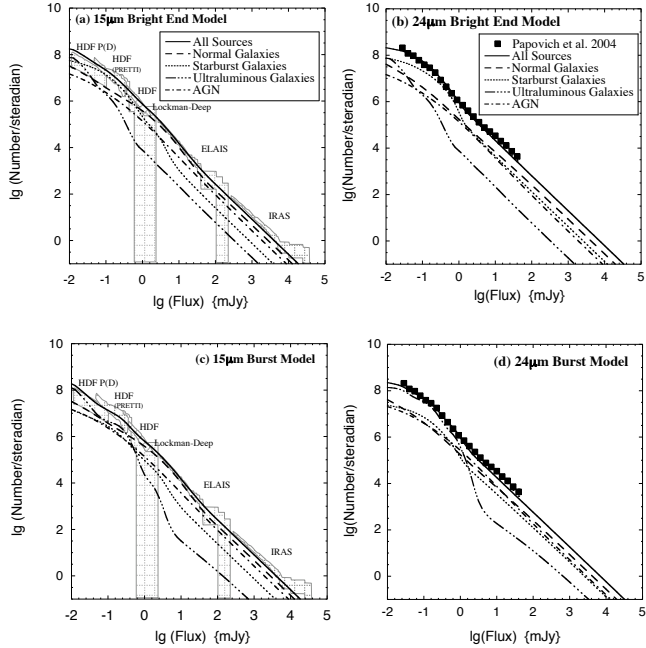


Figure 9. Model fits (sources per steradian) to the ISO 15 μm counts and the *Spitzer* 24 μm for the *Bright End Model* and the *Burst Model* described in the text. ISO 15 μm counts are from Hubble Deep Field (P(D) analysis - Oliver et al. (1997), HDF counts derived using the PRETTI method - Aussel et al. (1999), Lockman Hole - Elbaz et al. (1998), ELAIS - Serjeant et al. (2000) and shifted IRAS counts. 24 μm counts are from Papovich et al. (2004)

5 DISCUSSION AND CONCLUSIONS

We have investigated the photometric pre-selection method of high- z ULIRGs at $z = 1 - 2$, by focusing on the silicate absorption feature at 9.7 μm in the rest-frame. This technique requires observations only at MIR wavelengths, and is therefore very efficient and self-consistent. Applying our silicate-break technique to the sample of Charmandaris et al. (2004) we have tentatively identified the first candidate silicate-break galaxy at $z = 1.6$.

With *Spitzer*, we could select ULIRGs at $z \sim 1.5$ as silicate-break galaxies with $\log(f_{24}/f_{70}) < -1.7$. This colour cut is applicable to the selection of optically thick ULIRGs; i.e. the selection is biased towards high optical depth, although the sample is free from the contamination from quiescent star-forming galaxies. A more complete selection of silicate-break galaxies is possible with the IRS peak-up imagers with additional photometry at 70 μm to remove the contamination from quiescent star-forming galaxies at $z < 1$.

With *ASTRO-F*, a similar selection criteria of silicate-break galaxies to that of the IRS imagers is possible with L24 and L20W bands. The advantage of *ASTRO-F* is the larger field-of-view (100 arcmin^2) for these bands, compared to that of the IRS peak-up imagers, allowing for larger samples of silicate-break galaxies.

The proposed selection criteria is useful to construct samples of heavily obscured galaxies at $z = 1 - 2$. The majority of such galaxies are likely to be powered by starbursts rather than AGN. Therefore, such samples could be used to place strong limits on the star formation activity at $z = 1 - 2$. Note that spectroscopic redshifts might be difficult to

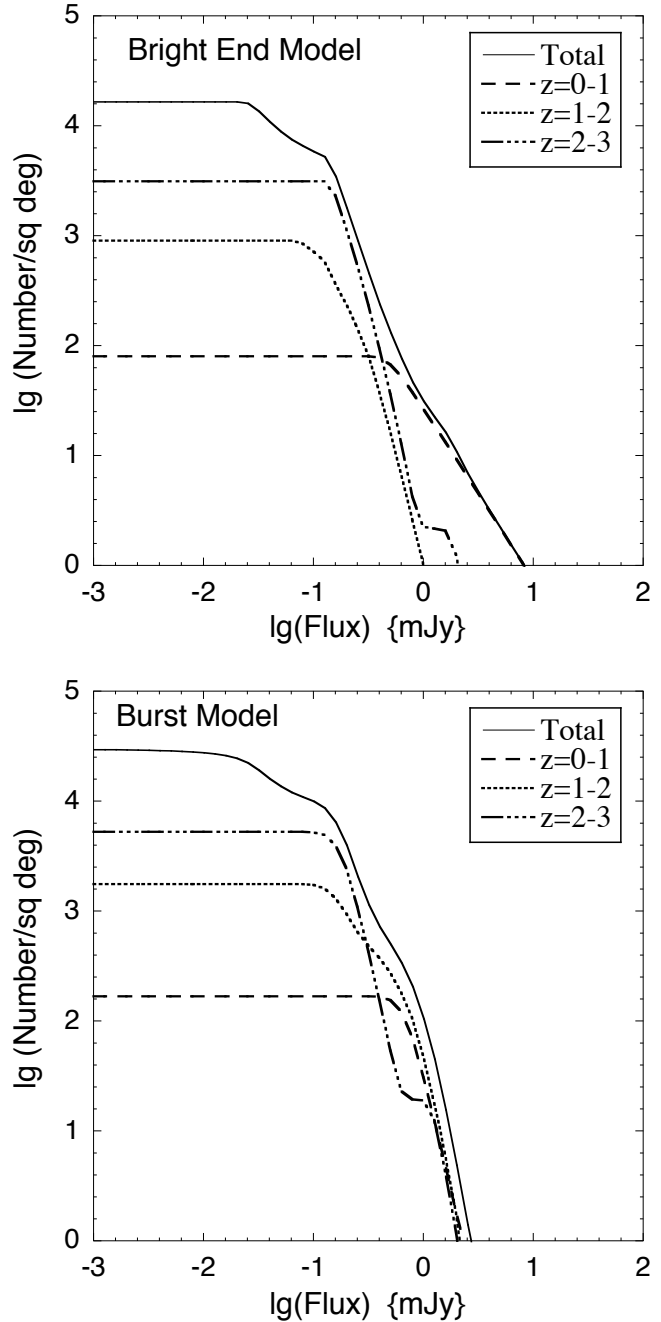


Figure 10. Predicted number of ULIRGs for the Bright End and Burst evolutionary models, as a function of redshift (sources per square degree). Numbers are divided into redshift bins of $z = 0 - 1$, $1 - 2$, and $2 - 3$. The selection criteria for the silicate-break effect dictates that the interesting sources will be ULIRGs between $z = 1 - 2$.

measure for such heavily obscured galaxies, which are expected to be faint at optical wavelengths. Furthermore, the expected redshift range of silicate-break galaxies overlaps with the so-called ‘redshift desert’, in which strong emission lines are not accessible from the ground. Thus, the proposed silicate-break selection method could play important role to investigate the nature of infrared galaxies at $z > 1$ bridging the gap between the IRAS-ISO and SCUBA populations.

In the *ASTRO-F* NEP surveys, we expect to detect \sim

400 – 1500 candidates of silicate-break galaxies depending on the evolutionary model. This large sample will allow us to derive important characteristics of ULIRGs at $z = 1 - 2$, such as their luminosity and spatial correlation function. Such data sets can also discriminate or tightly constrain multi-component number count models.

The available filters on *Spitzer* and *ASTRO-F* are found to be too broad to use individual PAH emission features for photometric pre-selections. Similarly, we find that the *ISO* 15 μm band is too broad to produce the colour anomaly for galaxies at $z \sim 0.5$, owing to the silicate absorption. Thus, using the silicate-break method, *Spitzer* and *ASTRO-F* can provide the first opportunity to pre-select high- z infrared galaxies with MIR bands.

ACKNOWLEDGMENTS

We thank S. Serjeant for useful and stimulating discussions. Also, we thank H. Hanami for useful comments, which improved the paper. We would like to thank D. Elbaz and H.W.W. Spoon for providing us with the observed spectra of galaxies. We are also grateful to D. Dale for distributing the SED template on the Web. We thank the referee for stimulating comments. CPP acknowledges a Fellowship to Japan from the European Union.

REFERENCES

Armus L. et al., 2004, ApJS, 154, 178

Aussel H., Cesarsky C.J., Elbaz D., Starck J.L., 1999, A&A, 342, 313

Blain A.W. et al., 2002, Physics Reports, 369, 111 (astro-ph/0202228)

Blain A.W., Chapman S., Smail I., Ivison R.J., 2004, ApJ, 611, 725

Chapman S.C., Blain A.W., Ivison R.J., Smail I.R., 2003, Nature, 422, 695

Chapman S.C., Smail I., Blain A.W., Ivison R.J., 2004, ApJ, 614, 671

Charmandaris V. et al., 2004, ApJS, 154, 142

Chary R., Elbaz D., 2001, ApJ, 556, 562

Cimatti A. et al., 2004, Nature, 430, 184

Cowie L.L., Hu E.M., 1998, ApJ, 502, 99

Dale D.A., Helou G., Contursi A., Silbermann N.A., Kolhatkar S., 2001, ApJ, 549, 215

Dickinson M., Papovich C., Ferguson H.C., Budavari T., 2003, ApJ, 587, 25

Dole H. et al., 2004, ApJS, 154, 93

Eales S., Lilly S., Gear W., Dunne L., Bond J.R., Hammer F., Le Fevre O., Crampton D., 1999, ApJ, 515, 518

Egami E. et al., 2004, ApJS, 154, 130

Elbaz D. et al., 1998, in Proc. of 34th Liege International Astrophysics Colloquium on the “Next Generation Space Telescope”, Belgium, June 1998, p.42

Elbaz D., Cesarsky C.J., Chanial P., Aussel H., Franceschini A., Fadda D., Chary R.R., 2002, A&A, 384, 848

Fadda D. et al., 2002, A&A, 383, 838

Fazio G.G. et al., 2004, ApJS, 154, 10

Fontana A. et al., 2003, ApJ, 594, 9

Fukugita M., Hogan C.J., & Peebles P.J.E., 1998, ApJ, 503, 518

Gear W.K., Lilly S.J., Stevens J.A., Clements D.L., Webb T.M., Eales S.A., Dunne L., 2000, MNRAS, 316, L51

Houck J.R. et al., 2004, ApJS, 154, 18

Huang J.-S. et al., 2004, ApJS, 154, 44

Hughes D. et al., 1998, Nature, 394, 241

Laurent O. et al., 2000, A&A, 359, 887

Le Floc'h E. et al., 2004, ApJS, 154, 170

Lilly S.J., Eales S.A., Gear W.K., Hammer F., Le Fevre O., Crampton D., Bond J.R., Dunne L., 1999, ApJ, 518, 641

Lonsdale C.J. et al., 2003, PASP, 115, 897

Lonsdale C.J. et al., 2004, ApJS, 154, 54

Matsuura H., Pearson C.P., 2004, in preparation

Matute I. et al., 2002, MNRAS, 332, L11

Murakami, H., 1998, Japanese infrared survey mission IRIS (ASTRO-F), In: Bely P.Y., Breckinridge J.B. (Ed), Space Telescopes and Instruments, Proc. SPIE 3356, 471

Oliver S.J. et al., 1997, MNRAS, 289, 471

Papovich C. et al., 2004, ApJS, 154, 70

Pearson C.P., Rowan-Robinson M., 1996, MNRAS, 283, 174

Pearson C.P., 2001, MNRAS 325, 1511

Pearson C.P., Matsuura H., Onaka T., Watarai H., Matsumoto T., 2001, MNRAS, 399, 1014

Pearson C.P. et al., 2004, MNRAS, 347, 1113

Pearson C.P., 2004, MNRAS, in preparation

Pearson C.P., Matsuura H., 2004, in preparation

Pozzi F. et al., 2004, ApJ, 609, 122

Rieke G.H. et al., 2004, ApJS, 154, 25

Rigopoulou D. et al., 1999, AJ, 118, 2645

Rowan-Robinson M., 2001, ApJ, 549, 745

Rowan-Robinson M. et al., 2004, MNRAS, 351, 1290

Sanders D.B., Mirabel I.F., 1996, ARA&A, 34, 725

Schechter P.L., Dressler A., 1987, AJ, 94, 563

Calzetti D., Storchi-bergmann T., 1997, AJ, 114, 592

Serjeant S.B.G. et al., 2000, MNRAS, 316, 768

Smail I., Ivison R.J., Blain A.W., 1997, ApJ, 490, L5

Smail I., Ivison R.J., Blain A.W., Kneib J.-P., 2002, MNRAS, 331, 495

Steidel C.C., Adelberger K.L., Shapley A.E., Pettini M., Dickinson M., Giavalisco M., 2003, ApJ, 592, 728

Simasaku K. et al., 2003, ApJ, 586, L111

Spoon H.W.W. et al., 2004a, ApJS, 154, 184

Spoon H.W.W., Moorwood A.F.M., Lutz D., Tielens A.G.G.M., Siebenmorgen R., Keane J.V., 2004b, A&A, 414, 873

Sturm E., Lutz D., Tran D., Feuchtgruber H., Genzel R., Kunze D., Moorwood A.F.M., Thornley M.D., 2000, A&A, 358, 481

Taniguchi Y. et al., 2003, ApJ, 585, 97

Takagi T., Arimoto N., Hanami H., 2003a, MNRAS, 340, 813

Takagi T., Vansevičius V., Arimoto N., 2003b, PASJ, 55, 385

Takagi T., Hanami H., Arimoto N., 2004, MNRAS in press(astro-ph/0405322)

van Dokkum P.G. et al., 2004, ApJ, 611, 703

Wada T. et al., 2003, Infrared Camera (IRC) on board ASTRO-F, In Mather J.C. (Ed), IR Space Telescopes and Instruments, Proc. SPIE, 4850, 179

Werner M.W. et al., 2004, ApJS, 154, 1

Xu C., Lonsdale C.J., Shupe D.L., Franceschini A., Martin C., Schiminovich D., 2003, ApJ, 587, 90